Evaluating the Assumptions in an Empirical Jet-Surface Interaction Noise Model

Cliff Brown*

NASA Glenn Research Center, Cleveland, OH, 44135, USA

A set of empirical jet-surface interaction noise models, developed for single-stream round nozzles exhausting over a simple surface in a static ambient, are evaluated for use in more realistic applications that include multi-stream nozzle systems, multi-plane surface geometries, and a flight-stream. The simple-single-stream models have several advantages when used in system-level noise studies: they are robust, they are quickly computed, and they are generally applicable to a wide range of configurations. However, these models require simplifying assumptions when applied to more complex jet exhaust systems. For example, previous work on multi-stream jets used an empirical formula to compute a single-stream equivalent jet potential core length that could be used to predict the noise using simple-single-stream jet-surface interaction models. This paper considers the effect of flight and multi-plane surfaces using a similar approach: introducing assumptions to simplify the complex system, applying the simple-single-stream models, and evaluating the uncertainty.

I. Introduction

The noise produced by an aircraft is a primary consideration in the overall design. Historically, the engine noise and airframe noise have been treated as separate entities. However, with the evolution to ultra-high bypass-ratio engines and the advent of integrated engine/airframe designs that seek higher operational efficiency, this approach to noise predictions is no longer sufficient. Noise prediction tools need to include jet-surface interaction (JSI), which includes noise produced by the jet exhaust passing near the airframe surfaces and the shielding or reflection of the jet-mixing noise by the airframe surfaces, to facilitate system-level design decisions that effect the noise, weight, range, and efficiency of an aircraft.

The NASA Commercial Supersonics Technology Project has pursued a Technical Challenge to design a propulsion system on a low-boom supersonic aircraft able to meet the ICAO Chapter 4 regulations for airport noise with 10 EPNdB cumulative margin to justify further development of the concept.[1] The Project used a multi-discipline approach to this problem employing system-level engine simulation software[2] to optimize the engine architecture and cycle, empirical and CFD based noise prediction models, and scale-model tests[3,4] to validate the predications and improve the models.

Empirical models are computationally efficient and are generally accurate over a specific range of variables. In many cases, this range may be extended by simplifying the flow or geometry, assuming the relative importance of various details, so that low-order models can be used to solve more advanced problems. These lower-order models have a few potential advantages: (1) they can be more general, (2) they can be more computationally efficient, (3) and they can be more mathematically robust than higher-order models. However, these advantages come with a trade-off; the predictions may have too much uncertainty for a particular study because of the simplifying assumptions required. Therefore, it is important to document the assumptions applied and the uncertainty created by using the model under these assumptions.

Empirical models have been developed for the JSI noise source and the shielding of jet-mixing noise effect for a simple flat surface near a single-stream round jet.[5–7] These simple-single-stream (SSS) JSI models rely on the jet-potential core length to nondimensionlize the flow at the surface trailing-edge and the source source distribution for the JSI source and shielding effect models respectively. The JSI-SSS models have been previously tested using multi-stream jets with simple surfaces by assuming an equivalent set single-stream jet parameters to compute the jet-potential core length;[8] this approach was shown to predict the

*Research Engineer, Acoustics Branch, 21000 Brookpark Rd., AIAA Member.

JSI noise source spectra reasonably well but over-predict the shielding effect. These JSI-SSS models are now evaluated for use in configurations with multi-planar surfaces, multi-stream nozzle systems and flight effects using an extensive model-scale dataset acquired at the NASA Glenn Research Center's Aero-Acoustics Propulsion Laboratory.[4]

II. Concept Aircraft and Experimental Data

The concept aircraft that motivates this study is shown in Figure 1a. This 3-engine supersonic concept has engines above (center) and below (outboard) the airframe. The center engine sits in a wedge between the angled tail fins and near an aft-deck; this arrangement offers the potential for some engine noise shielding. The outboard engines sit on pylons located near the edge between the aft-deck, toward the aircraft centerline, and the tail fin. The tail fin angles away from the outboard engine so that only about half the jet is covered by the airframe.

Two distinct planforms were required to estimate the aircraft propulsion noise: one for the center engine and one for the outboard engine. These planforms could rotate around the engine so that the microphone array was at the flyover ($\phi = 0$) or sideline ($\phi = 60^\circ$ and $\phi = 300^\circ$) observer locations (Figure 2). Note that the outboard engine requires two rotations to account for the effect of the left and right engine separately at the lateral observer location.

The three-engine configuration was designed to shield the engine noise from the center engine while meeting the performance and thrust balance requirements with two outboard engines. Therefore, three aft-decks were tested with the center engine planform to investigate the relationship between deck length and jet noise shielding; these planforms are shown in in Figures 3a, 3b, and 3c. Noise shielding is not possible considering the placement of the outboard engines so only one planform length was tested[a]; the outboard engine planform is shown in Figure 3d.

Three nozzle systems, designed to cover three distinct engine architectures, were tested with the various aircraft planforms. First, the IVP01 nozzle used a larger center plug that eliminated any flow from the inner stream to simulate an internally mixed flow turbo-fan engine. Second, the IVP44 nozzle, using most of the same hardware but with a smaller center plug, simulated the exhaust of a two-stream inverted velocity profile (IVP) separate flow engine. Finally, the IVP19 nozzle represents a three-stream split-tip flow nozzle exhaust system. Table 1 gives relevant exit areas for these nozzle systems. Note that the IVP01 and IVP44 systems required the third-stream nozzle to interface with the jet rig but it was neutralized by matching the exit velocity to the flight velocity.

The jet exit conditions tested were defined by the nozzle pressure ratio (NPR) on each stream and nozzle total temperature ratio (NTR) on the first and second streams. Each jet exit condition, assigned a setpoint number for easier reference, corresponds to the throttle setting on a proposed engine cycle and an aircraft flight speed. These engine cycles were selected from a NASA study to optimize aircraft range while still meeting the ICAO Chapter 4 noise certification with 10 EPNdB cumulative margin. Tables 2, 3, and 4 define the setpoints for the IVP01, IVP44, and IVP19 nozzle systems respectively. More details on the experimental setup and a summary of results can be found in Reference [4].

Table 1: Primary, secondary, and tertiary areas for the IVP01, IVP44, and IVP19 nozzle systems.[4]

Nozzle ID	A_2, in^2	A_1, in^2	A_3, in^2	A_1/A_2	LSF
IVP01	17.35	0.2	4.18	0	14.00
IVP44	12.33	5.41	0	0.44	14.00
IVP19	17.35	3.22	4.18	0.19	11.84

[a]Engine noise may be reflected to the flyover and lateral observers from the outboard engine. However, the surface length was expected to have a minimal impact on the reflected noise so additional lengths were not considered in the interest of test time.

(a) CST Concept

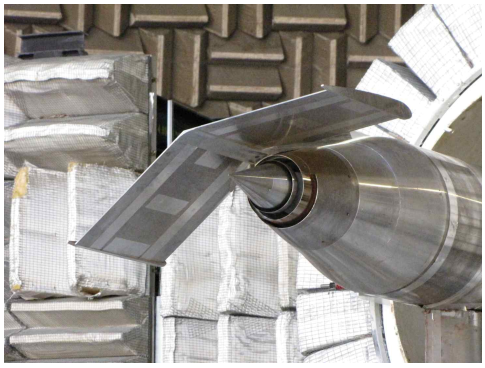

(b) Installed Test Setup

Figure 1: A NASA Commercial Supersonic Transport Project concept aircraft featuring a 3-engine propulsion system with exhaust near aft surfaces (a) and the mock aft-deck installed in the AAPL at the NASA Glenn Research Center (b).

Table 2: Jet exit flow conditions for the IVP01 engine configuration.[4] Note that NPR_3 was set to match the flight stream velocity.

Setpoint ID	Throttle, %	NPR_2	NPR_1	NPR_3	NTR_2	NTR_1	M_f
355	100	1.778	1.100	1.064	1.538	1.000	0.30
354	100	1.778	1.100	1.064	1.538	1.000	0.25
356	100	1.778	1.100	1.064	1.538	1.000	0.35

Table 3: Jet exit flow conditions for the IVP44 engine configuration.[4] Note that NPR_3 was set to match the flight stream velocity.

Setpoint ID	Throttle, %	NPR_2	NPR_1	NPR_3	NTR_2	NTR_1	M_f
210	60	1.464	1.658	1.000	1.513	1.193	0.0
220	70	1.553	1.685	1.000	1.553	1.201	0.0
230	80	1.578	1.872	1.000	1.599	1.237	0.0
240	90	1.658	1.908	1.000	1.653	1.245	0.0
250	100	1.775	1.844	1.000	1.704	1.239	0.0
250	100	1.775	1.844	1.000	1.704	1.239	0.0
250	100	1.775	1.844	1.000	1.704	1.239	0.0
215	60	1.464	1.658	1.064	1.513	1.193	0.30
225	70	1.553	1.685	1.064	1.553	1.201	0.30
235	80	1.578	1.872	1.064	1.599	1.237	0.30
245	90	1.658	1.908	1.064	1.653	1.245	0.30
255	100	1.775	1.844	1.064	1.704	1.239	0.30
254	100	1.775	1.844	1.045	1.704	1.239	0.25
256	100	1.775	1.844	1.091	1.704	1.239	0.35

Table 4: Jet exit flow conditions for the IVP19 engine configuration.[4]

Setpoint ID	Throttle, %	NPR_2	NPR_1	NPR_3	NTR_2	NTR_1	M_f
120	70	1.553	1.685	1.685	1.553	1.201	0.0
130	80	1.578	1.872	1.872	1.599	1.237	0.0
140	90	1.658	1.908	1.908	1.653	1.245	0.0
150	100	1.775	1.844	1.844	1.704	1.239	0.0
125	70	1.553	1.685	1.685	1.553	1.201	0.30
135	80	1.578	1.872	1.872	1.599	1.237	0.30
145	90	1.658	1.908	1.908	1.653	1.245	0.30
155	100	1.775	1.844	1.844	1.704	1.239	0.30
154	100	1.775	1.844	1.844	1.704	1.239	0.25
156	100	1.775	1.844	1.844	1.704	1.239	0.35

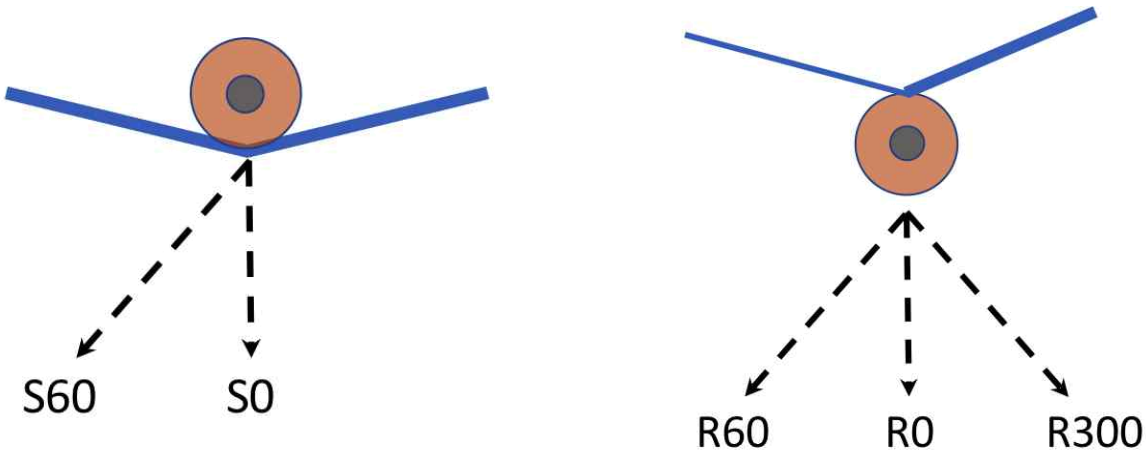

(a) Center Engine

(b) Outboard Engine

Figure 2: Observer angles tested via planform rotations during the JSI16 entry at the NASA Glenn Research Center[4] for the center and outboard engines.

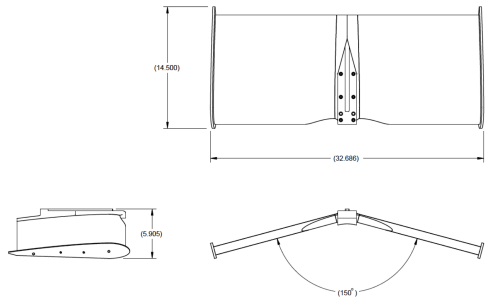

(a) Center Engine - Short Planform

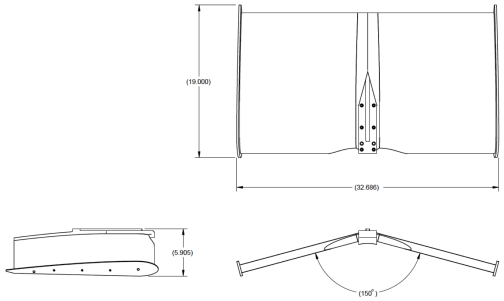

(b) Center Engine - Medium Planform

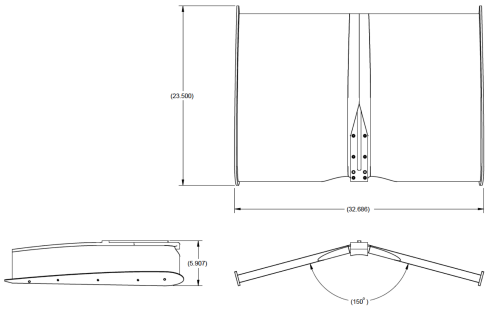

(c) Center Engine - Long Planform

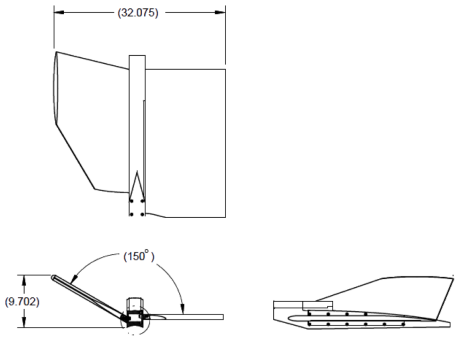

(d) Outboard Engine Planform

Figure 3: Model-scale planforms tested during the JSI16 entry at the NASA Glenn Research Center.[4]

III. Model Predictions

Empirical jet-surface interaction (JSI) noise models have been used to predict the installed exhaust noise for the center and outboard engines at the flyover and lateral observer locations. The jet-surface configurations show in Section II present two sources: the jet-mixing noise, produced by the high-speed turbulent flow mixing with the ambient atmosphere, and the jet-surface interaction source, produced by turbulent eddies passing near/over the trailing edge of the aft-deck. The surface effects the jet-mixing noise by either blocking (shielding) it from the observer or reflecting it back toward the observer. The JSI system uses separate models[5,6,8] for each source and effect; this limits the scope of each model and makes the system more flexible and robust. The framework used by the empirical models is expressed mathematically as:

$$PSD_T = (PSD_M + G_{S/R}) \oplus PSD_D \tag{1}$$

where PSD_M is the jet-mixing noise, $G_{S/R}$ is the shielding/reflection effect, and PSD_D is the jet-surface interaction (JSI) noise source. The symbol $\oplus$ indicates addition on a sound power basis and $+$ indicates addition on a logarithmic (dB) basis. Empirical models have been developed for PSD_D and $G_{S/R}$ using data from a round single-stream jet near a flat semi-infinite surface. While there are some empirical models for the jet-mixing noise of IVP nozzles (e.g. Stone model in ANOPP[9]), the experimentally measured jet-mixing noise (PSD_M) will be used to reconstruct PSD_T in this work to better evaluate only the JSI source and shielding/reflecting effect models.

The empirical models are based on experimental data acquired using a semi-infinite flat plate near a single stream round jet. These restrictions in the underlying dataset require making several assumptions to predict the noise for multi-stream jets with multi-plane surface geometries. First, the multi-stream jet flow is assumed to behave like a single-stream jet where the temperature and velocity are equal to the mass-weighted average across all streams. In particular, the JSI models nondimsionalize the axial peak and decay of the jet turbulence (P_D) and the axial noise source distribution ($G_{S/R}$) by the jet potential core length. In a single-stream jet, this nondimensionalization is reliable over a large range of subsonic jet Mach numbers and temperature ratios. However, nondimensionalizing by the potential core length in a multi-stream jet is less

reliable because the range and number of engine parameters make it difficult to model. Previous work using the jet potential core length model described in Reference [10] with conventional separate flow engines for JSI noise predictions suggests that it collapses the turbulence profile reasonably well but that the jet mixing noise source distribution is more varied.[8] Nevertheless, this potential core length model is used again here assuming that these 2- and 3-stream inverted velocity profile engines can be modeled as single-stream jets defined by the mass-weighted averaged velocity and temperature values.

The second assumption relates to the surface: the surfaces, shown in Figure 3, are not semi-infinite. The center engine planform might reasonably be assumed semi-infinite because the tail fins may shield the lateral observer from the jet noise. However, the outboard engine planform features only a partial span over the jet which leaves less surface to reflect noise to the observers and less surface trailing-edge length exposed to the jet flow than assumed in the model[b] that Combined, the assumptions required to predict the noise from the center and outboard engines at the flyover and lateral observer locations push the model well outside the range of surfaces for which it was developed.

Finally, the empirical JSI models assume that the engine is static and, therefore, do not include flight effects. A flight stream may change the jet potential core length, change the noise source distribution, or change the directivity of the JSI noise sources. Additionally, the empirical model employed to predict the jet potential core length used by the models also assumes a static jet. Flow data acquired from these nozzle systems show that the flight stream lengthens the jet potential core relative to a static jet but has a relatively small effect on the distribution of jet mixing noise sources in the jet.[4] Thus, the JSI noise source prediction, which relies on the flow velocity and turbulence at the surface trailing-edge, may be more affected under the static engine assumption than the shielding or reflection effect predictions as they depend more on the noise source distribution.

The empirical noise prediction framework, as expressed in Equation 1, produces PSD for any specified observer angle. Internally, the models actually predict PSD on a 1-foot radius arc without atmospheric attenuation (i.e. 1-foot lossless condition) at the model-scale used in the original experiments.[11,12] These predictions can then scaled to account for observer distance, atmospheric conditions, and nozzle diameter. Because these models are designed to predict the noise in a system-level design environment, these PSD predictions must be transformed into effective perceived noise levels (EPNL).

EPNL is a system-level metric used in aircraft certification. EPNL is a integrated value, in time and frequency, of spectra measured at defined locations and weighted by frequency to account for the human response to different frequencies. EPNL values are computed from the total predicted PSD (PSD_T in Equation 1) by: (1) transforming from model- to full-scale, (2) transforming to observer points corresponding to a level aircraft flyover at 1000-feet altitude while applying atmospheric attenuation for standard day conditions, (3) Doppler-shifting the spectra while transforming observer angles to flyover time using the flight Mach number (M_f), (4) applying the perceived noise level weighs to correct for the human perception of sound, and (5) integrating the 1/3-octave spectra in frequency and time. Note that the flight Mach number matching the flight stream (M_f) was used to calculate the EPNL values except in the static where $M_f = 0.3$ was assumed to compute the flyover.

III.A. EPNL Predictions

Figure 4 shows EPNL as a function of setpoint for the IV44 nozzle system (inverted velocity profile, two-stream, separate flow). In each case, defined as a combination of engine, surface length, and observer, the EPNL increase is nearly linear as setpoint number increases. This behavior is captured by the model; in most cases the modeled EPNL increases approximately linearly with a similar slope to the experimental data. However, the modeled data has an offset to the measured EPNL that depends on surface length and observer angle. Furthermore, this offset does not always capture the trend shown in the data. Figure 4a, for example, shows the center engine planform at the flyover observer angle ($\phi = 0$) for three surface lengths; where measured EPNL is very similar for the short, medium, and long surface, with the medium giving the lowest line, the modeled data monotonically decreases from short to long. At the sideline observer location, the model performs better for the center engine planform, which can be reasonably assumed semi-infinite (Figure 4b) than at the outboard engine location (Figure 4c) which features a partial span. Note that the outboard planform predictions are the same for $\phi = 60°$ and $\phi = 300°$ as the model is symmetric and does

[b]Finite span empirical models have been developed for symmetric configurations (see [7] for details). Because the outboard engine planform extends only to one side of the engine, the models must assume either that the span is semi-infinite or that the span is finite but symmetric about the nozzle.

not distinguish between ±60°. Finally, the EPNL predictions in Figure 4 are near the data in the static and $M_f = 0.3$ cases even though flight effects are not included in the empirical models. This indicates that most of the flight effect is captured by changes in the jet mixing (isolated) noise. This does not necessarily mean that the JSI noise source is not effected by the flight stream but this source may have only a small influence on the EPNL once the scale factor is applied.

The IV19 nozzle system is an inverted velocity profile separate flow nozzle with a partial third stream. Figure 5 compares predictions from the empirical JSI models with measure data for the center and outboard engine planforms. Note that only a subset of possible setpoint/planform combinations were run during the experiment. First, Figure 5a shows comparisons for the center engine planform, medium length surface, with and without flight effect. Similar to the IV44 nozzle system, the prediction follows the linear trend shown in the data but with an offset; the prediction is about 2 EPNdB high in the static case and about 3 EPNdB high in the $M_f = 0.3$ case. At $\phi = 60°$ (Figure 5b) the predictions follow the trend shown in the data as setpoint increases but are again high by 1.5-2 EPNdB. Note that these points all have a $M_f = 0.3$ flight stream that is included in the jet-mixing noise but not as a parameter in the JSI noise models. Finally, the predictions for the outboard planform at $\phi = 60°$ and $\phi = 300°$ have an offset to the data but the data is 1.5-2 EPNdB above the predictions. Overall, the predictions follow the trend with increasing setpoint but have a near constant offset from the data.

The JSI model does not include flight effects, which are solely captured in the jet-mixing noise, but this trend holds at $M_f = 0.3$ with similar offsets. Figure 6 shows the variation of EPNL for $0.25 \leq M_f \leq 0.35$ for the IV44 nozzle (setpoints 154-156). Over this range, the EPNL computed from the data decreases approximately linearly with increasing flight Mach number and the model captures a similar slope (although it is offset by ±2 EPNdB depending on surface length and observer. A similar result is obtained with the center engine planform, lateral observer, for the IVP19 nozzle system although the offset is greater (on the order of 3 EPNdB) and there is a small slope change in the data between $0.3 \leq M_f \leq 0.35$. The predicted EPNL as a function of flight speed for the IV19, outboard engine, has a similar offset range to the data as the other cases but the slope between $0.25 \leq M_f \leq 0.3$ is too negative. However, the slope is generally consistent with the data across the range $0.25 \leq M_f \leq 0.35$ for these cases which indicates that the effect of flight has a relatively small role in the JSI predictions and the static engine assumption is reasonable or, at least, not the largest source of uncertainty for these engines.

Finally, Figure 8 shows how EPNL changes as a function of flight Mach number for the IV01 nozzle system. This nozzle system, which simulates a mixed-flow turbofan engine, was tested at a limited number of setpoints to provide a comparison to the inverted velocity profile nozzles. Similar to the IV44 and IV19 nozzle systems, the predicted EPNL for the IV01 has an offset to the measured value ranging from approximately 3 EPNdB for the center engine, short planform at the flyover observer to -2 dB for the outboard engine at $M_f = 0.35$. However, unlike the IV44 and IV19 nozzles, the predicted EPNL does not generally capture the slope as flight Mach number increases. This may be in indication that the noise source distribution is more affected by the flight stream with this nozzle system or that the models do not account for the effects of the larger center plug. Whatever the cause, these comparisons show that while neglecting the effect of flight was a reasonable assumption for the IV44 and IV19 nozzles, this result may not be general and more work is required in this area.

The EPNL was predicted at two observer locations for three different nozzle systems across a wide range of flow conditions using two distinct aircraft planforms. These predictions required assuming that (1) the 2- and 3- stream nozzles could be modeled as equivalent single-stream jets, (2) the multi-planar finite surfaces could be modeled as semi-infinite flat plates, and (3) the effect of flight on the JSI noise is negligible. These predictions are within 3 EPNdB of the experimental validation data in every case and with 2 EPNdB for most cases. Given the assumptions in the predicted values, this seems like a good result. However, in most cases the variation in the experimental data between nozzle system and engine cycle were within 3 EPNdB;[4] the models' uncertainty, therefore, is on the same order as the variations they are supposed to predict. As a result, more work is needed to improve the models for system-level optimization with multi-stream engines, complex surfaces, and flight effects.

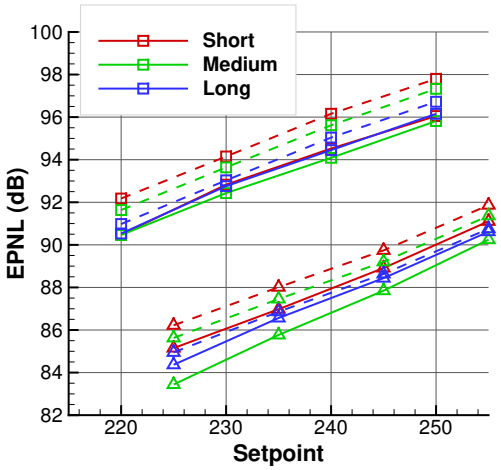

(a) Center - $\phi = 0$

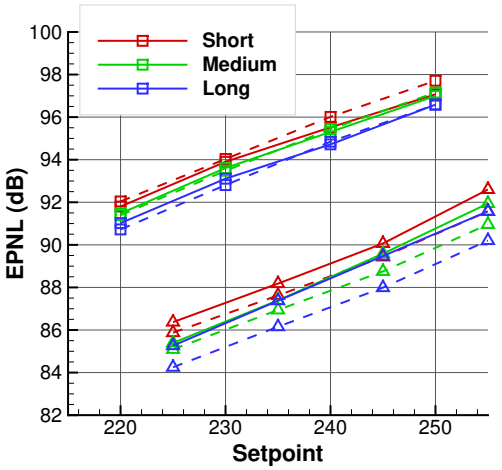

(b) Center - $\phi = 60°$

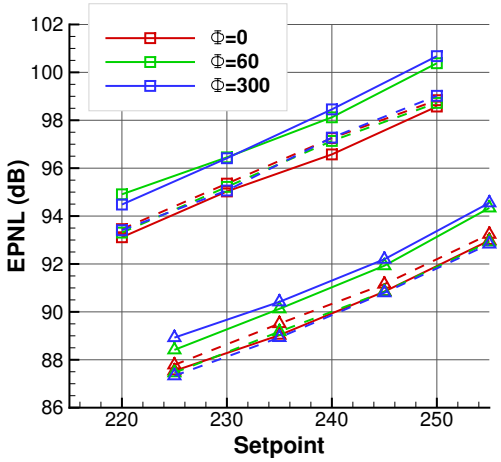

(c) Outboard

Figure 4: EPNL as a function of setpoint for the IVP44 nozzle system at static ($M_f = 0$, squares) and $M_f = 0.3$ (triangles) flight speeds. Solid lines represent measured data and dashed lines represent the prediction results.

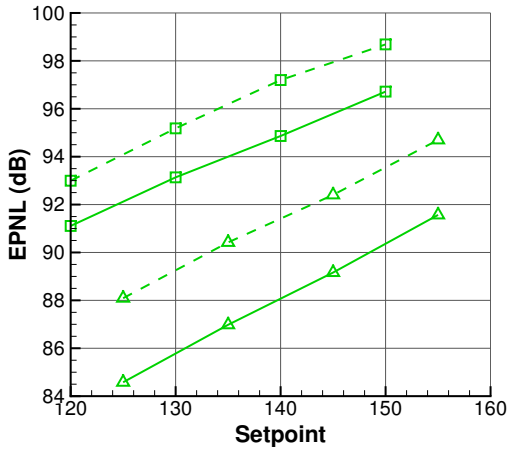

(a) $\phi = 0$

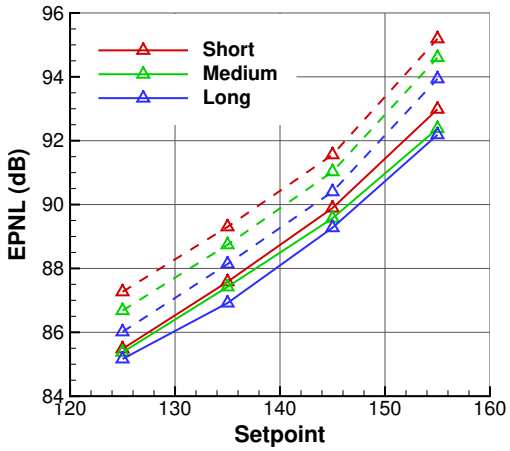

(b) $\phi = 60°$

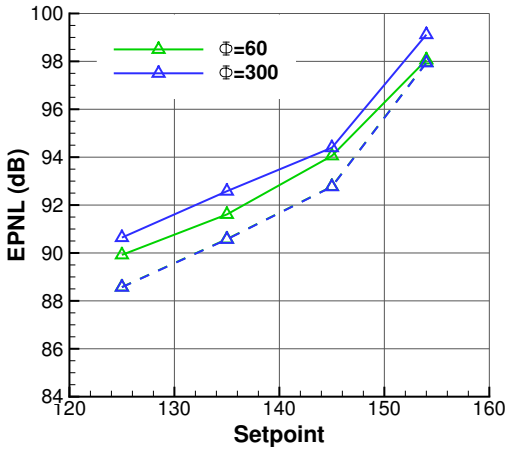

(c) Outboard

Figure 5: EPNL as a function of setpoint for the medium surface as a function of setpoint for the IVP19 nozzle system, center engine at $M_f = 0$ (squares) and $M_f = 0.3$ (triangles). Solid lines represent measured data and dashed lines represent the prediction results.

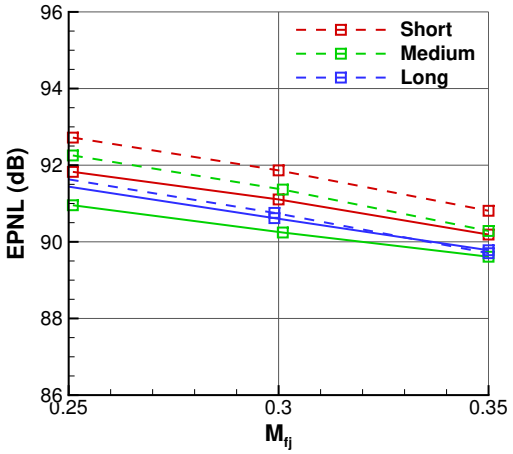

(a) Center - $\phi = 0$

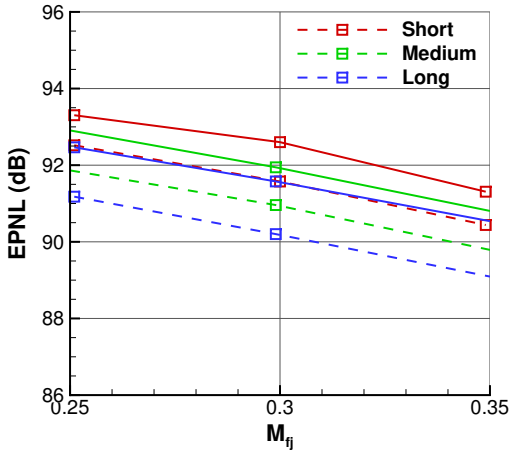

(b) Center - $\phi = 60°$

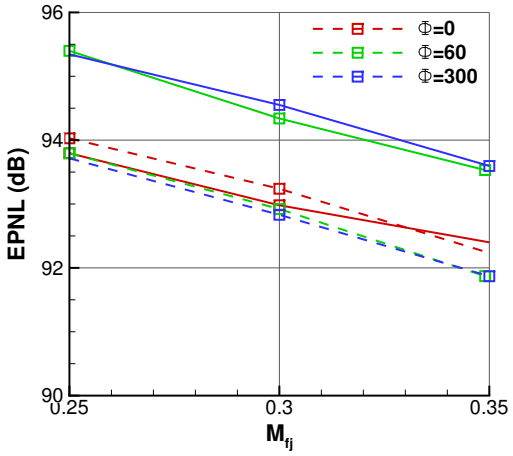

(c) Outboard

Figure 6: EPNL as a function of flight Mach number at setpoints 154/155/156 (Table 3) for the IVP44 nozzle system. Solid lines represent measured data and dashed lines represent the prediction results.

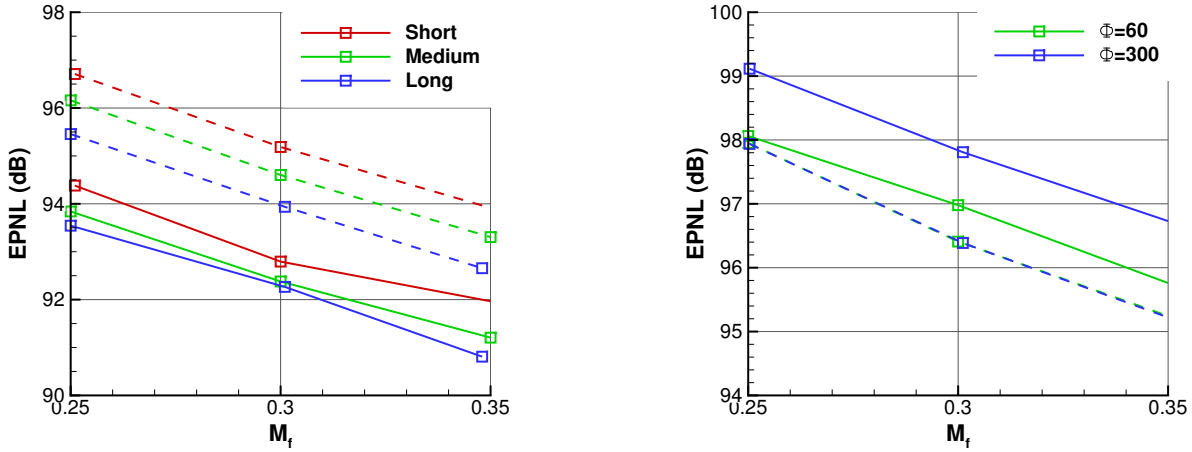

(a) Center

(b) Outboard

Figure 7: EPNL as a function of flight speed for the IVP19 nozzle system center and outboard engine planforms at setpoints 154, 155, 156 measured at the lateral observer location ($\phi = 60°$). Solid lines represent measured data and dashed lines represent the prediction results.

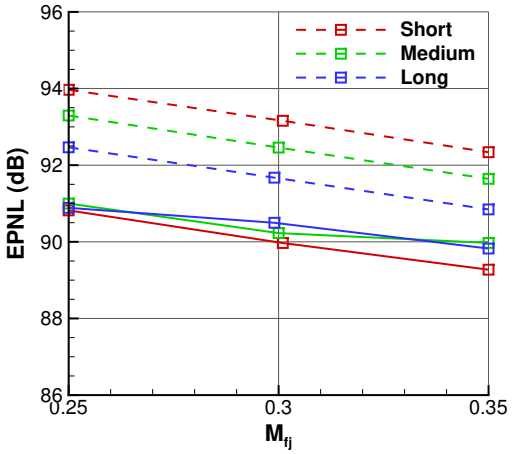

(a) Center - $\phi = 0$

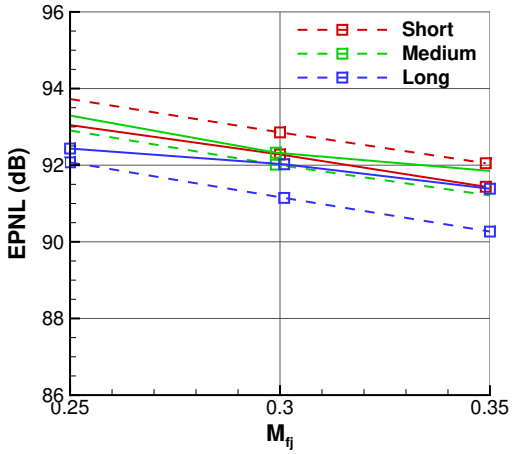

(b) Center - $\phi = 60°$

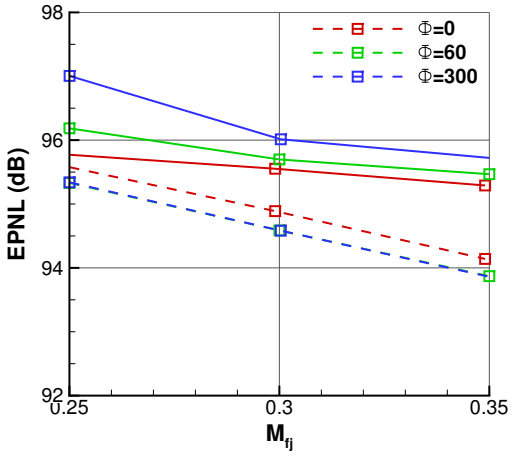

(c) Outboard

Figure 8: EPNL as a function of flight Mach number at setpoints 154/155/156 (Table 2) for the IVP01 nozzle system. Solid lines represent measured data and dashed lines represent the prediction results.

III.B. Spectral Predictions

The spectral predictions used to compute the EPNL in Section III.A are created from three separate components: the JSI noise model, the shielding/refection effect model, and the jet-mixing noise. EPNL, however, is an integrated value which makes it impossible to determine how each component contributes to the overall level and uncertainty in the result. Therefore, it is useful to compare the spectral predictions with the experimentally measured spectra to determine where the models fail and identify the best areas for improvement. Furthermore, the experimental data can be separated into JSI noise source, shielding/reflecting effects, and jet-mixing noise components[13] that compare directly to the model output. Note that the experimentally measured jet-mixing noise (isolated/no surface configuration) was used in all spectral predictions so there is no model to evaluate for that component.

Each model contributes to a different frequency range in the overall prediction: the jet-mixing noise model provides the broadband spectral base, the JSI noise model provides the low-frequency increase, and the shielding/reflecting model modifies the mid- to high-frequencies. For example, Figure 9 compares the measured and predicted 1/3-octave spectra from the IV44 nozzle system at setpoint 250 for the center engine, medium planform, and outboard engine at the flyover and lateral observer locations. First, for the center engine (Figures 4a-4b), the predicted spectra agrees with the measured data to within ±2 dB across most angles and frequencies; this is, in part, because the measured jet-mixing noise was used to create the prediction. At low frequencies, and particularly at upstream to broadside angles[c], the noise is a combination of the jet-mixing noise and JSI noise. Again, the prediction is within about ±2 dB near and above the JSI peak frequency. The model predicts a JSI spectra that is somewhat wider than measured increasing the difference on the low-frequency side of the peak. The most significant differences are at high-frequencies and, particularly, downstream angles; this frequency range for the center engine is predicted by the jet-mixing noise combined with the shielding effect model. The model predicts very little shielding at downstream angles where is a significant reduction in the measured data leading the model to overpredict the sound level.

Figures 9c and 9d show the same comparison but for the outboard engine. Again, the broadband and low frequencies, represented by the jet-mixing noise and JSI noise, are predicted within approximately ±2 dB. However, the predicted noise in high frequency range measured by the flyover observer ($\phi = 0$, Figure 9c) is within the ±2 dB range, unlike the center engine, while the model underpredicts the high frequency noise for the lateral observer ($\phi = 0$, Figure 9d) by 3-5 dB. This difference at high frequencies, where the refection model is active, is interesting for two reasons: (1) the partial span appears less important at the flyover observer and (2) "perfect" reflection of incoherent sources should only increase the noise by 3 dB so the 3-5 dB differences suggests that the surface may not just reflect the jet-mixing noise but also modify the sources (and these sources are "visible" to the lateral observer due to the partial span). There is evidence that the surface can modify the jet-mixing noise[4,15] but these mechanisms then to increase rather than decrease the noise. As a result, the mechanism behind the change observed here is not yet known.

Figure 10 compares predicted and modeled spectra for the same model system with $M_f = 0.3$ (setpoint 255). The flight stream in this case reduces the discrepancy at the high frequencies for both the center and outboard planform at both flyover and lateral observer locations. Phased-array source localization data shows that the flight effect did not significantly change the source distribution in these cases despite elongating the jet potential core.[4] Thus, if the source distribution is substantially the same as the static case and the model does not include any flight speed information, the improved prediction is due to the changes in the jet-mixing noise. This further suggests that the surface has some effect on the jet-mixing noise beyond the trailing-edge noise and that effect appears to be reduced by the flight stream in this case.

The largest discrepancies between the predicted and measured spectra are in the frequency range where shielding and reflection models play a significant role. Returning briefly to Section III.A, EPNL is not a simple integration of the spectra but is weighted for the human response to hearing after transforming from model- to full-scale. As a result, the shielding and reflection models will tend have an outsized impact on the ENPL; the frequency range where they work are more likely to be among the most penalized in the EPNL calculation[d]. Conversely, the frequencies most effected by the JSI noise are likely to be below the most penalized EPNL frequencies and, therefore, matter less in the overall integration. This non-uniform weighting is important to remember when looking at each model's performance in isolation and when considering where

[c]The JSI noise has a peak amplitude around $\theta = 90°$ while the jet-mixing noise increases downstream to become a more dominant source

[d]See Reference [4] for a more complete discussion of annoyance weightings and EPNL using this test hardware.

to devote resources toward improving predictions at the system-level.

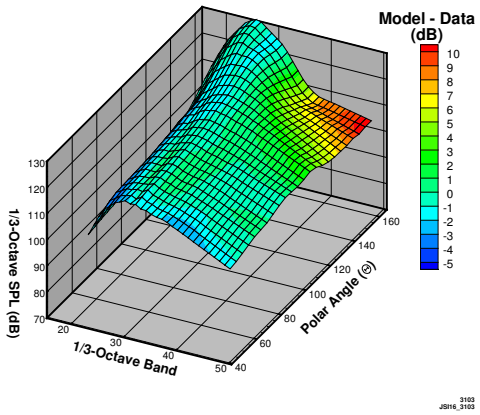

(a) Center, $\phi = 0$

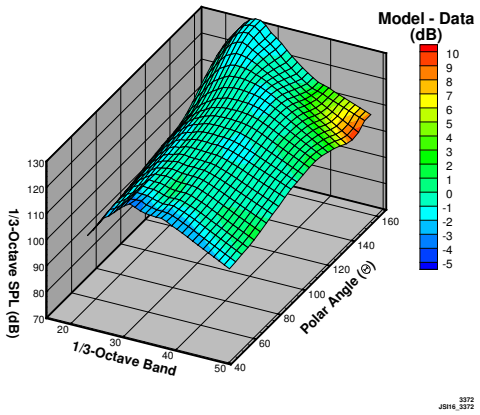

(b) Center, $\phi = 60°$

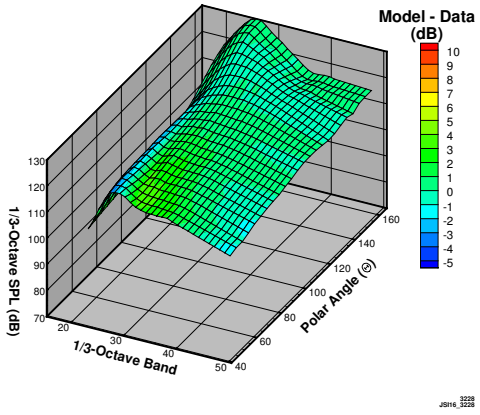

(c) Outboard, $\phi = 0°$

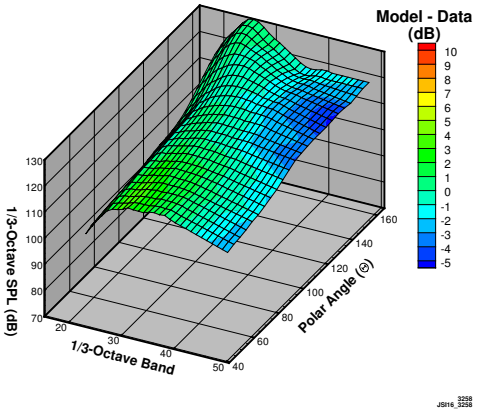

(d) Outboard, $\phi = 60°$

Figure 9: Comparison between spectral prediction and measured data for the IV44 center engine/medium planform and outboard engine planform at $\phi = 0$ and $\phi = 60°$. The engines are operating at setpoint 250 ($M_f = 0$). Note that the surface shape is defined by the model and positive values on the color bar indicate that the model is over-predicting the noise levels.

III.B.1. Shielding Model

The shielding model is based on the fundamental assumption that sound is blocked based on line-of-sight path to the observer; if the observer can not see the source then some portion of the sound will be shielded. In this line-of-sight model, the spatial relationship between the source location and surface trailing-edge is critical. Phased-array source localization data from subsonic single-stream jets shows that source location is a linear function of $log_{10}(f)$ if source location is nondimensionalized by jet potential core length.[14] Thus, the empirical shielding model assumes a linear relationship between the shielding (G_S) and logarithmic frequency as:

$$G_S(f) = C_1 + C_2\, log_{10}(f) \tag{2}$$

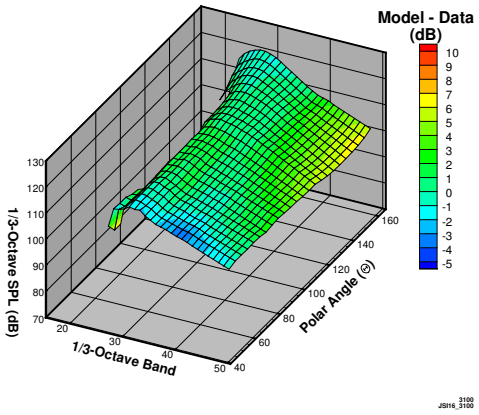

(a) Center, $\phi = 0$

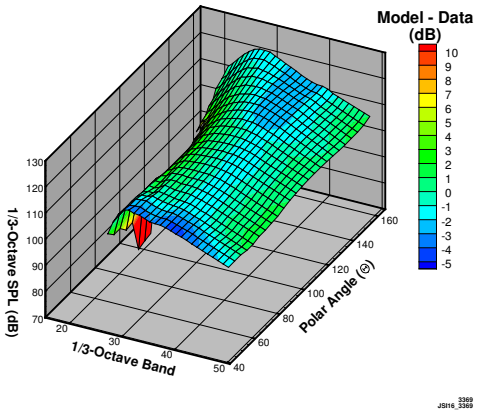

(b) Center, $\phi = 60°$

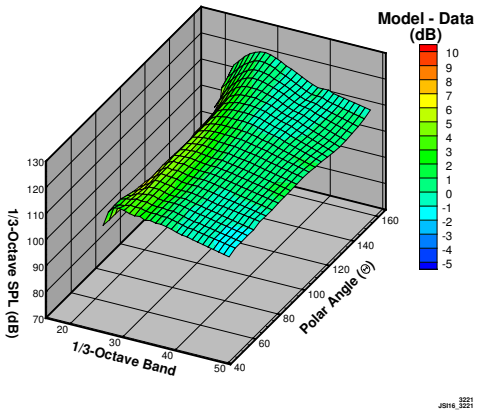

(c) Outboard, $\phi = 0°$

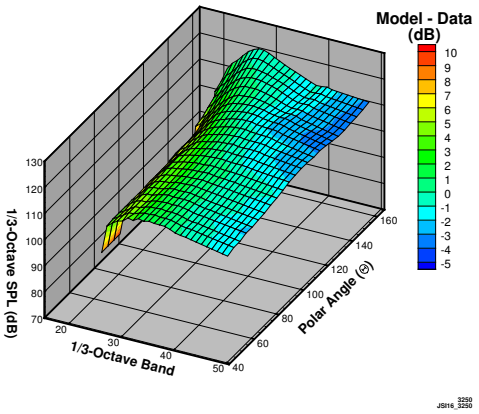

(d) Outboard, $\phi = 60°$

Figure 10: Comparison between spectral prediction and measured data for the IV44 center engine/medium planform and outboard engine planform at $\phi = 0$ and $\phi = 60°$. The engines are operating at setpoint 255 ($M_f = 0.3$). Note that the surface shape is defined by the model and positive values on the color bar indicate that the model is over-predicting the noise levels.

where C_1 and C_2 are constants determined by fitting data to secondary equations[e]. The data fitting process attempts to account for factors that violate the strict line-of-sight model by determining the coefficients that best fit the data. Critically, the data used to determine these coefficients is from a single-stream round jet without a center plug and, therefore, the model assumes that the source distribution varies according to standard scaling rules (e.g. area, velocity, etc.) to all classes of jets.

Jet potential core length is a key parameter used to nondimensionalize the shielding model. However, the potential core length model[10] used with these inverted velocity profile multi-stream jets was actually developed for conventional (i.e. not inverted) jet and has a much greater uncertainty than the single-stream models. Although a known source of potentially significant uncertainty, this potential core length model is the best available for this class of jet and, therefore, is used for these predictions while recognizing (1) the importance of this parameter in the shielding model and (2) that the IVP may significantly change on the sources and their distribution in the jet relative to even a standard two-stream nozzle architecture.

Figure 11 compares the shielding predicted using the empirical model to the shielding extracted from the measured spectra. The model performs reasonably well at $\theta = 60°$ and $\theta = 90°$, considering all the assumptions required, but fails at the downstream angles $\theta = 120°$ and $\theta = 150°$. The empirical shielding model assumes a simple single-stream jet, with one shear-layer between the jet and ambient, without a center plug. In contrast, the IV44 jet has a center plug, an inner warm stream, an outer hot, and a flight stream (depending on the setpoint). This model was used previously to predict the shielding effect on a conventional separate flow nozzle system (without flight).[8] In that case, phased-array data showed that the jet-mixing noise sources were actually farther downstream than anticipated (based on the single-stream model); as a result, the shielding effect was overpredicted. In this case, the shielding at downstream angles is underpredicted suggesting that the jet-mixing noise sources have moved upstream relative to the single-stream jet.

There are a few factors in the jet-surface system that complicate the line-of-sight assumption in shielding model for the single-stream jet and these factors become significantly more important in the case of multi-stream jets. First, model is nondimensionalized based on the location of the peak amplitude source at each frequency. There are, however, lower amplitude sources at all frequencies created throughout the jet (i.e. even if the peak source is 100% shielded the observer will still hear some noise at that frequency created by these secondary sources). The model, by using the jet-potential core length nondminensionalization for the peak amplitude sources, assumes these secondary sources scale similarly and allows the fitting process determine how many of these sound sources propagate to the observer. The multi-stream jet has two (or more) shear-layers originating at different axial locations and, therefore, very likely has a much different distribution of secondary sources than the single-stream jet.

A second factor not directly accounted for in the model is the refraction of sound around the surface trailing-edge. Refraction of sound is based on the location of the source source relative to the edges and the sound wavelength. Again, the model does not directly address this factor but allows the fitting process to account for the effect. Note, however, that the basic model produces PSD as a function of Strouhal number before transforming into frequency based on the actual requested geometry; this nondimensionalizes the model in frequency but breaks the direct connection to sound wavelength when scaling is applied. Also, refraction of sound depends on several additional parameters (e.g. trailing-edge shape or thickness) that are not included in the model. Therefore, the model may not include refraction effectively.

Finally, the presence of the surface near the jet can change the jet-mixing noise itself. For example, in some cases the peak turbulence intensity will occur in the shear-layer new formed downstream of the surface trailing edge rather than in the free-shear layer.[15] The model is based on the shielding effect extracted using using the independently measured jet noise and, therefore, these changes will be included in the shielding model. Additionally, the effect of the surface on the jet-mixing noise may or may not scale the same way as the pure shielding effect. Ultimately, these effects likely require a separate model, incorporated into Equation 1, to fully capture.

[e]The coefficients C_1 and C_2 are actually modeled as linear equations with two coefficients each; these four coefficients are determined using an empirical fit to the data. See [6] for details.

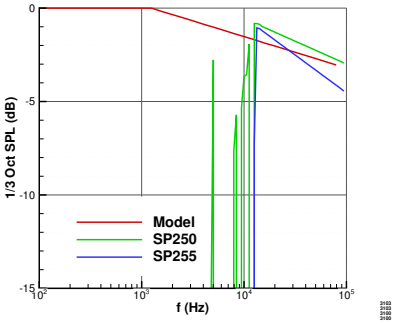

(a) $\theta = 60°$

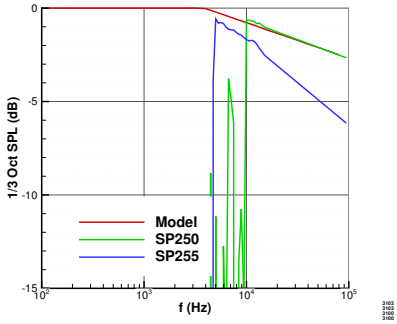

(b) $\theta = 90°$

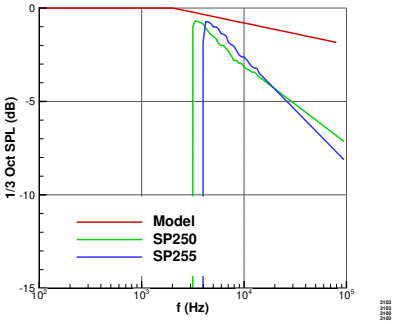

(c) $\theta = 120°$

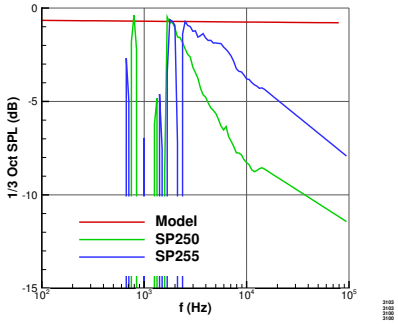

(d) $\theta = 150°$

Figure 11: Shielding computed using the empirical model and measured data for the IV44 center engine/medium planform at $\phi = 0$ and setpoints 250-255. Note the low large amplitude changes at lower frequencies in the extracted data result from the spectral extraction used to separate the shielding effect.

III.B.2. JSI Source Model

The jet-surface interaction noise source model estimates the sound spectra created when the turbulent jet flow passes near the trailing-edge of a surface and transitions from a wall/near-wall flow to to a free-shear layer flow[f]. The noise produced and "scattered" by the edge is dipolar in nature with the peak noise at approximately $\theta = 90°$ when $M_f = 0$. Spectrally, the JSI source appears as a low-frequency augmentation to the jet-mixing noise although it is, as shown in Equation 1, a distinct noise source. The empirical JSI noise model developed for single-stream jets near semi-infinite flat surfaces approximates the JSI spectra as parabolic in logarithmic frequency or:

$$P_d = C_1 + C_2 \, log_{10} \left(\frac{f}{F_{peak}} \right)^2 \tag{3}$$

where C_1 sets the peak amplitude, C_2 sets the spectral width, and F_{peak} set the peak frequency. Similar to the shielding model, C_1, C_2, and F_{peak} are modeled coefficients; each one has an underlying equation with coefficients fit to the data (see [5] for details). Also like the shielding model the jet-potential core length is the key nondimensionalizing parameter though for a different reason; it is used in the JSI model to collapse the velocity and turbulence profile relative to the trailing-edge location rather than source distribution. Finally, note that as a dipolar source the JSI noise scales with jet velocity (U) as U^6 compared to U^8 for jet-mixing noise. As a result, the JSI noise source contributes more to the total noise at lower jet velocities.

The JSI noise model assumes that (1) the surface is semi-infinite, (2) multi-stream jets can be approximated as single-stream jets with the same mass-weighted average velocity and temperature and (3) the effect of flight can be neglected. First, consider the effect of semi-infinite versus partial span surfaces. Figures 12a and 12c compare the predicted and measured spectra from the IV44 nozzle at setpoint 230[g] for the center and outboard planforms respectively. The center engine planform in this case can reasonably be assumed semi-infinite and the model underpredictes the total noise at upstream angles and low frequencies where the JSI source is most prominent (Figure 12a). The outboard engine planform features only a partial surface but the model, assuming that the surface is semi-infinite, produces a prediction closer to the data (Figure 12c. The prediction is the same for both planforms but the partial planform reduces the JSI noise in the measured data giving a better comparison. The model, if functioning properly, should more accurately predict the center engine spectra and overpredict the partial span outboard planform. Thus, the semi-infinite span assumption fails in this case.

Figure 13 shows the JSI spectra extracted from the total spectra for setpoint 230 in Figure 12 for the observer at $\theta = 90°$. The JSI model predicts the JSI spectra at $\theta = 90°$ and then assumes the theoretical directivity of a dipole in free-space to compute other observer angles so this is the key angle. The model underpredicts the peak amplitude and spectral width (on the high frequency side of the peak) for both the center and outboard planforms. In fact, the model appears to perform worse for the outboard planform indicating that the jet-mixing noise is contributing more to the overall noise in Figure 12c. Generally, this behavior indicates that (1) the JSI model is not properly accounting for all of the multi-stream effects (underpredicting center engine peak) and (2) the a semi-infinite surface span assumption will need to be addressed once properly accounting for multi-stream effects. However, addressing these assumptions in the model may not have a significant effect on the EPNL. The peak amplitude of these JSI noise spectra occurs between $800 \leq f \leq 1000$ Hz at model-scale (Figure 13) which becomes $55 \leq f \leq 75$ Hz at full-scale. These low frequencies are not heavily weighted in the EPNL calculation.

The JSI source model predicts the spectrum at $\phi = 0$ and $\theta = 90°$ and then uses the theoretical directivity for a dipole source in free-space to scale that spectra to observers at other polar and azimuthal angles. Figure 14 compares the predicted and measured spectra for the center engine/medium and outboard engine planforms at setpoint 230 for the sideline $\phi = 60°$ observer. The model is within ± 2 dB for the center engine/medium planform and ± 3 dB for the outboard engine planform at setpoint 230 in the low frequency region where the JSI noise source can be significant. Thus, it appears assuming the dipole directivity for azimuthal angles is not a limiting assumption at this point.

[f] JSI noise can also include 'scrubbing' noise created by the jet flow passing along the surface. However, far-field noise and phased-array source localization data showed the JSI noise was dominated by the trailing-edge source for the configurations used to develop the model. See [11] and [14] for details.

[g] Setpoints 230/235 were selected for this analysis because the lower jet velocity compared to setpoints 250/255 makes the JSI noise more prominent in the total spectra (i.e. not completely masked by the jet-mixing noise).

Figures 12b and 12d compare predictions with data the measured data for the same case with a $M_f = 0.3$ flight stream. Data were removed during processing when the measured level was within 1 dB of the independently measured background noise. As a result, it is impossible to quantify the effect of flight on the JSI noise model.

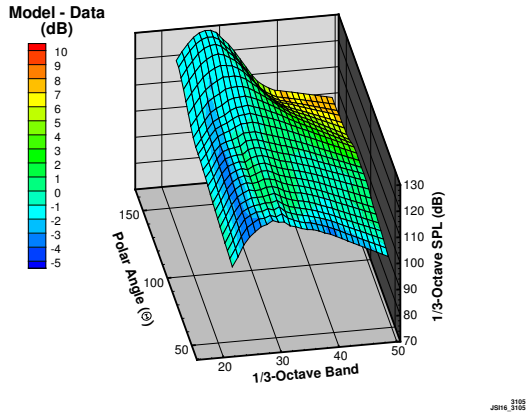

(a) Center, $M_f = 0$

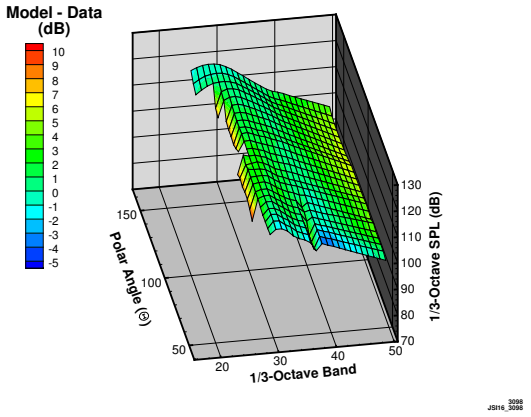

(b) Center, $M_f = 0.3$

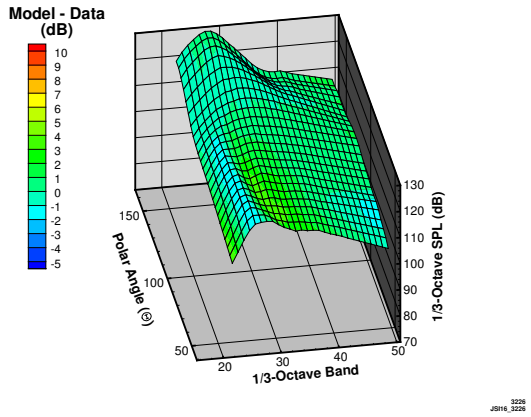

(c) Outboard, $M_f = 0$

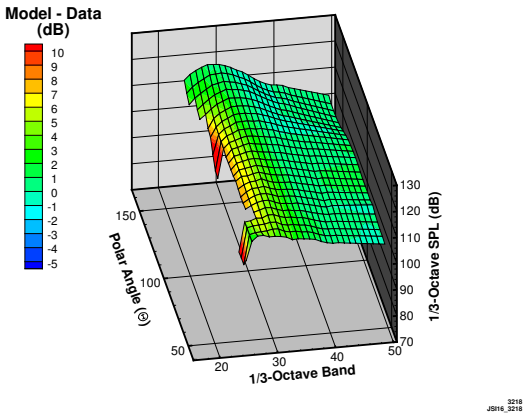

(d) Outboard, $M_f = 0.3$

Figure 12: Comparison between spectral predicted and measured spectra for the IV44 center engine planform (medium length) and outboard engine planform at $\phi = 0$. These spectra are at setpoints 230 and 235. Note that the surface shape is defined by the model and positive values on the color bar indicate that the model is over-predicting the noise levels; regions where the measured data is below the background noise has been removed.

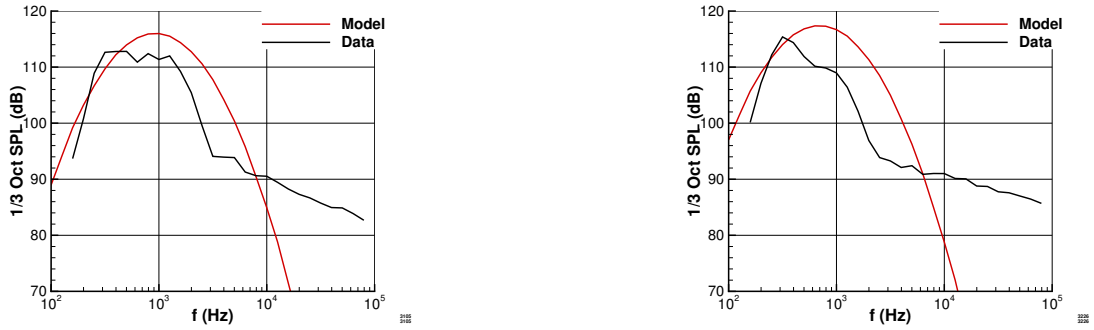

(a) Center (b) Outboard

Figure 13: JSI noise predicted using the empirical model and extracted from the measured data for the IV44 center engine/medium planform at $\theta = 90°$, $\phi = 0$ and setpoints 230.

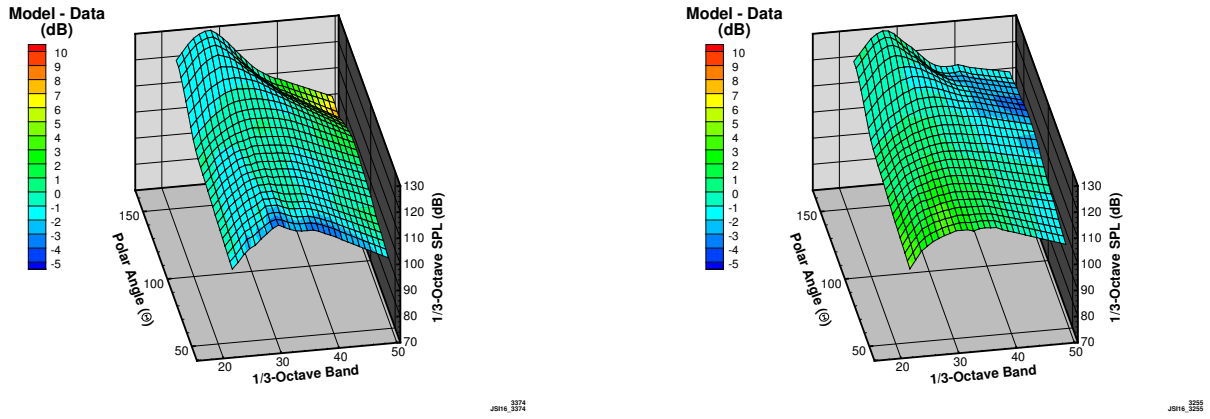

(a) Center (b) Outboard

Figure 14: Comparison between spectral prediction and measured data for the IV44 center engine/medium planform and outboard engine planform at $\phi = 60$. These spectra are at setpoint 230. Note that the surface shape is defined by the model and positive values on the color bar indicate that the model is over-predicting the noise levels; regions where the measured data is below the background noise has been removed.

III.B.3. IVP19 Nozzle

The IV19 nozzle system was the most complicated tested featuring an inverted velocity profile on the inner two streams and a third-stream covering only half the annulus. Experimental data were acquired for only a subset of the possible configurations with this nozzle but, as the most complex case, it is useful to evaluate the model performance on a spectral basis. Figure 15 compares spectral predictions with the measure data for the IV19 nozzle system at setpoint 155 for the center engine, medium length planform at $\phi = 0$ and $\phi = 60°$ and for the outboard engine planform at $\phi = 60°$. The center engine spectra a $\phi = 0$ (Figure 15a) shows differences between the predicted and measured spectra at high frequencies similar to those found with the IV44 nozzle but at different angles - more at broadside and upstream angles - caused by the shielding model. At $\phi = 60°$, the prediction for the center engine is better across most frequencies and angles but the model (1) underpredicts the noise at high-frequencies and the farthest downstream angles and (2) overpredicts the noise at low frequencies and angles $60° \leq \theta \leq 100°$ (Figure 15b). The underprediction at high frequencies results from the shielding model issues discussed above. The overprediction at low frequencies, which is worse for the outboard engine (Figure 15c), originates in the JSI source model.

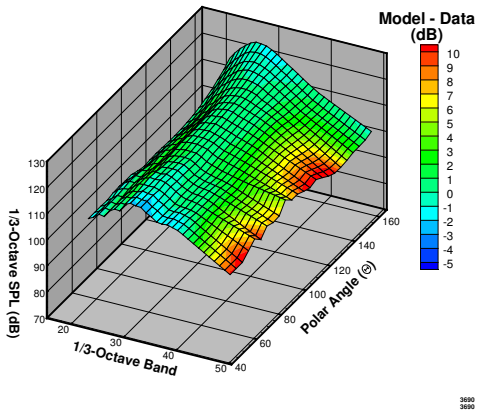

(a) Center, $\phi = 0$

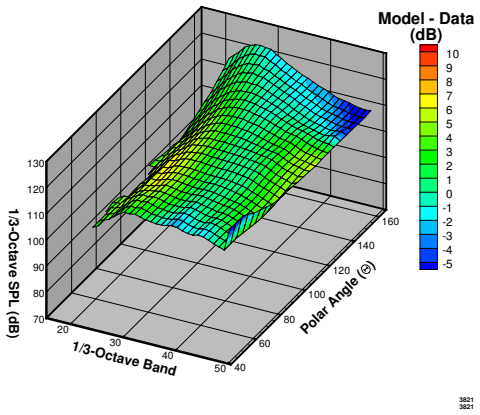

(b) Center, $\phi = 60°$

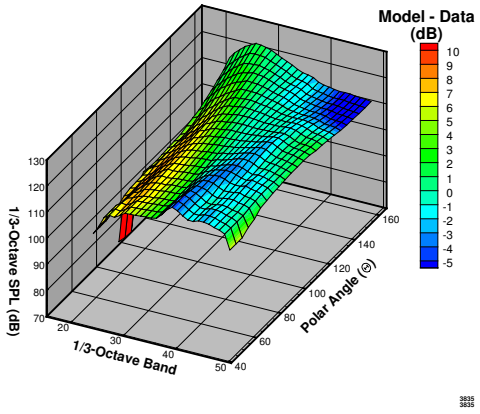

(c) Outboard, $\phi = 60°$

Figure 15: Prediction versus measured data[4] for the IVP19 nozzle system at setpoint 155. Note that shape of the surface is defined by the model and positive values on the color bar indicate that the model is over-predicting the noise levels.

IV. Summary

Empirical models have been used to predict the jet-surface interaction noise exhaust noise for a concept aircraft. These models have been designed for iterative system-level studies and, therefore, optimized to minimize computation time using several simplifying assumptions. These assumptions are now being evaluated using recently acquired experimental data from a scale-model of the engine and aft deck of the concept vehicle. The particular assumptions addressed are (1) that the multi-planar aircraft geometry is a flat surface, (2) multi-stream nozzle systems can be reasonably modeled as single-stream jets using mass-weighted average values and (3) that the effect of flight on the JSI noise and effects is small. Effective Perceived Noise Levels (EPNL) were computed for the center and outboard engine planforms using the experimentally acquired data and the spectra predicted by the model. The comparisons vary depending on the exact geometry and flow condition but the predictions were generally accurate to approximately ± 2 EPNdB. This uncertainty is on the same order as the variations across the entire range of hardware tested and, therefore, unacceptably high. A comparison of the underlying spectra showed that the largest source of error in the EPNL is caused by the shielding model; specifically, the likely shift of source locations and possible new sources related to the multi-stream nozzle system not present in a single-stream jet. Further spectral analysis show discrepancies in the jet-surface interaction noise source related to partial-span surfaces (outboard engine planform) and azimuthal observer angle (i.e. sideline versus flyover); the semi-infinite surface assumption seems to be the most likely source of these issues. However, the JSI source is sufficiently low in frequency that it does not have a large impact on EPNL at full-scale so it is a secondary concern to the shielding model if system-level EPNL computations are the primary use for the model. Finally, the inclusion of flight effects does not appear to have a large impact on the accuracy of the model. Overall, this analysis suggests that addressing the assumptions of source location in the shielding model first and then the partial span effects in the JSI source model will lead to the most improvement.

Acknowledgements

This work was supported by the NASA Advanced Air Vehicle Program, Commercial Supersonic Technology Project.

References

[1]Bridges, J. Brown, C., Seidel, J., "NASA's Pursuit of Low-Noise Propulsion for Low-Boom Commercial Supersonic Vehicles", in 54^{th} *AIAA Aerospace Sciences Meeting*, AIAA SciTech Forum 2018, 2018.

[2]Huff, D.L. et. al., "Perceived Noise Analysis for Offset Jets Applied to Commercial Supersonic Aircraft", AIAA 2016-1635, 2016.

[3]Bridges, J.E., Podboy, G.G., Brown, C.A., "Testing Installed Propulsion For Shielded Exhaust Configurations", AIAA 2016-3042, 2016.

[4]Bridges, J., "Aeroacoustic Validation of Installed Low Noise Propulsion for NASA's N+2 Supersonic Airliner", in 54^{th} *AIAA Aerospace Sciences Meeting*, AIAA SciTech Forum 2018, 2018.

[5]Brown, C., "An Empirical Jet-Surface Interaction Noise Model with Temperature and Nozzle Aspect Ratio Effects", AIAA 2015-0229, 2015.

[6]Brown, C., "Empirical Models for the Shielding and Reflection of Jet Mixing Noise by a Surface", AIAA 2015-3128, 2015.

[7]Brown, C., "Including Finite Surface Span Effects in Empirical Jet-Surface Interaction Noise Models", AIAA 2016-0006, 2016.

[8]Brown, C., Podboy, G., Bridges, J., "Modeling Jet-Surface Interaction Noise for Separate Flow Nozzles", AIAA 2016-2862, 2016.

[9]Stone, J.R., Krejsa, E.A., Clark, B.J., Burton, J.J., "Jet Noise Modeling for Suppressed and Unsuppressed Aircraft in Simulated Flight", NASA/TM 2009-215524, 2009.

[10]Bridges, J., "Simple Scaling Of Multi-Stream Jet Plumes For Aeroacoustic Modeling", AIAA 2016-1637, 2016.

[11], Brown, C., "Jet-Surface Interaction Test: Far-Field Noise Results", ASME GT2012-69639, 2012.

[12]Brown, C.A. , "Jet-Surface Interaction Test: Far-Field Noise Results", J. Eng. Gas Turbines Power, **1**35(7), Jun. 2013.

[13]Brown, C., "Developing an Empirical Model for Jet-Surface Interaction Noise", AIAA 2014-0878, 2014.

[14]Podboy, G., "Jet-Surface Interaction Test: Phased Array Noise Source Localization Results", ASME GT2012-69801, 2012.

[15]Brown, C., Wernet, M., "Jet-Surface Interaction Test: Flow Measurement Results", AIAA 2014-3198, 2014.